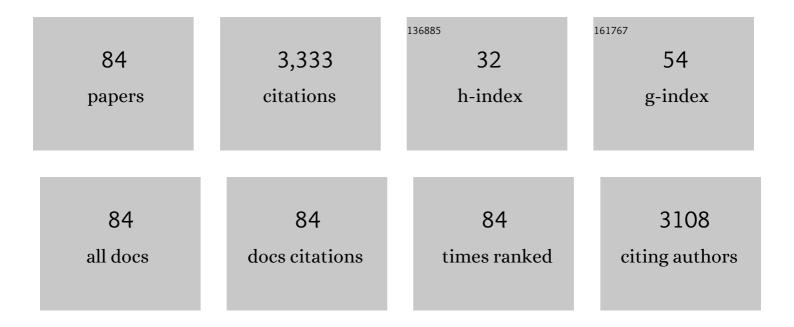
Moritz H Albrecht

List of Publications by Year in descending order

Source: https://exaly.com/author-pdf/4773348/publications.pdf Version: 2024-02-01



#	Article	IF	CITATIONS
1	Effects of Spaceflight on Astronaut Brain Structure as Indicated on MRI. New England Journal of Medicine, 2017, 377, 1746-1753.	13.9	235
2	Cinematic Rendering in CT: A Novel, Lifelike 3D Visualization Technique. American Journal of Roentgenology, 2017, 209, 370-379.	1.0	152
3	Coronary CT Angiography–derived Fractional Flow Reserve. Radiology, 2017, 285, 17-33.	3.6	152
4	Epicardial adipose tissue density and volume are related to subclinical atherosclerosis, inflammation and major adverse cardiac events in asymptomatic subjects. Journal of Cardiovascular Computed Tomography, 2018, 12, 67-73.	0.7	143
5	Review of Clinical Applications for Virtual Monoenergetic Dual-Energy CT. Radiology, 2019, 293, 260-271.	3.6	133
6	Dual-Energy CT–based Display of Bone Marrow Edema in Osteoporotic Vertebral Compression Fractures: Impact on Diagnostic Accuracy of Radiologists with Varying Levels of Experience in Correlation to MR Imaging. Radiology, 2016, 280, 510-519.	3.6	130
7	Assessment of an Advanced Monoenergetic Reconstruction Technique in Dual-Energy Computed Tomography of Head and Neck Cancer. European Radiology, 2015, 25, 2493-2501.	2.3	121
8	Advanced image-based virtual monoenergetic dual-energy CT angiography of the abdomen: optimization of kiloelectron volt settings to improve image contrast. European Radiology, 2016, 26, 1863-1870.	2.3	120
9	Comprehensive Comparison of Virtual Monoenergetic and Linearly Blended Reconstruction Techniques in Third-Generation Dual-Source Dual-Energy Computed Tomography Angiography of the Thorax and Abdomen. Investigative Radiology, 2016, 51, 582-590.	3.5	115
10	State-of-the-Art Pulmonary CT Angiography for Acute Pulmonary Embolism. American Journal of Roentgenology, 2017, 208, 495-504.	1.0	86
11	Dual energy computed tomography virtual monoenergetic imaging: technique and clinical applications. British Journal of Radiology, 2019, 92, 20180546.	1.0	81
12	Influence of Coronary Calcium on Diagnostic Performance of Machine Learning CT-FFR. JACC: Cardiovascular Imaging, 2020, 13, 760-770.	2.3	73
13	Coronary CT angiography–derived plaque quantification with artificial intelligence CT fractional flow reserve for the identification of lesion-specific ischemia. European Radiology, 2019, 29, 2378-2387.	2.3	70
14	Update on Cardiovascular Applications of Multienergy CT. Radiographics, 2017, 37, 1955-1974.	1.4	68
15	lodine and Fat Quantification for Differentiation of Adrenal Gland Adenomas From Metastases Using Third-Generation Dual-Source Dual-Energy Computed Tomography. Investigative Radiology, 2018, 53, 173-178.	3.5	60
16	Virtual Noncalcium Dual-Energy CT: Detection of Lumbar Disk Herniation in Comparison with Standard Gray-scale CT. Radiology, 2019, 290, 446-455.	3.6	57
17	Virtual Monoenergetic Imaging and Iodine Perfusion Maps Improve Diagnostic Accuracy of Dual-Energy Computed Tomography Pulmonary Angiography With Suboptimal Contrast Attenuation. Investigative Radiology, 2017, 52, 659-665.	3.5	57
18	Prognostic implications of coronary CT angiography-derived quantitative markers for the prediction of major adverse cardiac events. Journal of Cardiovascular Computed Tomography, 2016, 10, 458-465.	0.7	56

MORITZ H ALBRECHT

#	Article	IF	CITATIONS
19	A noise-optimized virtual monoenergetic reconstruction algorithm improves the diagnostic accuracy of late hepatic arterial phase dual-energy CT for the detection of hypervascular liver lesions. European Radiology, 2018, 28, 3393-3404.	2.3	55
20	Extra-abdominal dual-energy CT applications: a comprehensive overview. Radiologia Medica, 2020, 125, 384-397.	4.7	50
21	Value of a noise-optimized virtual monoenergetic reconstruction technique in dual-energy CT for planning of transcatheter aortic valve replacement. European Radiology, 2017, 27, 705-714.	2.3	45
22	Dual-energy CT in patients with colorectal cancer: Improved assessment of hypoattenuating liver metastases using noise-optimized virtual monoenergetic imaging. European Journal of Radiology, 2018, 106, 184-191.	1.2	45
23	Monoenergetic Dual-energy Computed Tomographic Imaging. Journal of Thoracic Imaging, 2017, 32, 151-158.	0.8	43
24	Dual-energy CT in early acute pancreatitis: improved detection using iodine quantification. European Radiology, 2019, 29, 2226-2232.	2.3	42
25	Color-coded virtual non-calcium dual-energy CT for the depiction of bone marrow edema in patients with acute knee trauma: a multireader diagnostic accuracy study. European Radiology, 2020, 30, 141-150.	2.3	41
26	Endoleaks after endovascular aortic aneurysm repair: Improved detection with noise-optimized virtual monoenergetic dual-energy CT. European Journal of Radiology, 2017, 94, 125-132.	1.2	40
27	Evaluation of virtual monoenergetic imaging algorithms for dual-energy carotid and intracerebral CT angiography: Effects on image quality, artefacts and diagnostic performance for the detection of stenosis. European Journal of Radiology, 2018, 99, 111-117.	1.2	40
28	Noise-Optimized Virtual Monoenergetic Dual-Energy CT Improves Diagnostic Accuracy for the Detection of Active Arterial Bleeding of the Abdomen. Journal of Vascular and Interventional Radiology, 2017, 28, 1257-1266.	0.2	39
29	Coronary Computed Tomographic Angiography-Derived Fractional Flow Reserve Based on Machine Learning for Risk Stratification of Non-Culprit Coronary Narrowings in Patients with Acute Coronary Syndrome. American Journal of Cardiology, 2017, 120, 1260-1266.	0.7	37
30	Noise-optimized virtual monoenergetic dual-energy computed tomography: optimization of kiloelectron volt settings in patients with gastrointestinal stromal tumors. Abdominal Radiology, 2017, 42, 718-726.	1.0	35
31	Comparative evaluation of non-contrast CAIPIRINHA-VIBE 3T-MRI and multidetector CT for detection of pulmonary nodules: In vivo evaluation of diagnostic accuracy and image quality. European Journal of Radiology, 2016, 85, 193-198.	1.2	34
32	Coronary Computed Tomographic Angiography-Derived Fractional Flow Reserve for Therapeutic Decision Making. American Journal of Cardiology, 2017, 120, 2121-2127.	0.7	34
33	Artificial intelligence in bone age assessment: accuracy and efficiency of a novel fully automated algorithm compared to the Greulich-Pyle method. European Radiology Experimental, 2020, 4, 6.	1.7	34
34	High-pitch low-voltage CT coronary artery calcium scoring with tin filtration: accuracy and radiation dose reduction. European Radiology, 2018, 28, 3097-3104.	2.3	33
35	Impact of Coronary Computerized Tomography Angiography-Derived Plaque Quantification and Machine-Learning Computerized Tomography Fractional Flow Reserve on Adverse Cardiac Outcome. American Journal of Cardiology, 2019, 124, 1340-1348.	0.7	32
36	Noise-optimized advanced image-based virtual monoenergetic imaging for improved visualization of lung cancer: Comparison with traditional virtual monoenergetic imaging. European Journal of Radiology, 2016, 85, 665-672.	1.2	30

MORITZ H ALBRECHT

#	Article	IF	CITATIONS
37	Dual-energy CT of the heart current and future status. European Journal of Radiology, 2018, 105, 110-118.	1.2	29
38	Accuracy and Radiation Dose Reduction Using Low-Voltage Computed Tomography Coronary Artery Calcium Scoring With Tin Filtration. American Journal of Cardiology, 2017, 119, 675-680.	0.7	28
39	Dual-Energy Computed Tomography in Cardiothoracic Vascular Imaging. Radiologic Clinics of North America, 2018, 56, 521-534.	0.9	28
40	Diagnostic accuracy of quantitative dual-energy CT-based bone mineral density assessment in comparison to Hounsfield unit measurements using dual x-ray absorptiometry as standard of reference. European Journal of Radiology, 2020, 132, 109321.	1.2	28
41	Single- and dual-energy CT pulmonary angiography using second- and third-generation dual-source CT systems: comparison of radiation dose and image quality. European Radiology, 2019, 29, 4603-4612.	2.3	26
42	Dual-Energy Computed Tomography Virtual Monoenergetic Imaging of Lung Cancer. Journal of Computer Assisted Tomography, 2016, 40, 80-85.	0.5	25
43	Improved coronary artery contrast enhancement using noise-optimised virtual monoenergetic imaging from dual-source dual-energy computed tomography. European Journal of Radiology, 2020, 122, 108666.	1.2	25
44	Impact of noise-optimized virtual monoenergetic dual-energy computed tomography on image quality in patients with renal cell carcinoma. European Journal of Radiology, 2017, 97, 1-7.	1.2	24
45	Survival of patients with non-resectable, chemotherapy-resistant colorectal cancer liver metastases undergoing conventional lipiodol-based transarterial chemoembolization (cTACE) palliatively versus neoadjuvantly prior to percutaneous thermal ablation. European Journal of Radiology, 2018, 102, 138-145.	1.2	22
46	Modified calcium subtraction in dual-energy CT angiography of the lower extremity runoff: impact on diagnostic accuracy for stenosis detection. European Radiology, 2019, 29, 4783-4793.	2.3	22
47	Artificial intelligence machine learning-based coronary CT fractional flow reserve (CT-FFRML): Impact of iterative and filtered back projection reconstruction techniques. Journal of Cardiovascular Computed Tomography, 2019, 13, 331-335.	0.7	21
48	Diagnostic accuracy of low and high tube voltage coronary CT angiography using an X-ray tube potential-tailored contrast medium injection protocol. European Radiology, 2018, 28, 2134-2142.	2.3	20
49	Transarterial chemoembolization in pancreatic adenocarcinoma with liver metastases: MR-based tumor response evaluation, apparent diffusion coefficient (ADC) patterns, and survival rates. Pancreatology, 2018, 18, 94-99.	0.5	20
50	Traumatic bone marrow edema of the calcaneus: Evaluation of color-coded virtual non-calcium dual-energy CT in a multi-reader diagnostic accuracy study. European Journal of Radiology, 2019, 118, 207-214.	1.2	20
51	Diagnostic Accuracy of Noncontrast Self-navigated Free-breathing MR Angiography versus CT Angiography: A Prospective Study in Pediatric Patients with Suspected Anomalous Coronary Arteries. Academic Radiology, 2019, 26, 1309-1317.	1.3	20
52	Virtual non-calcium dual-energy CT: clinical applications. European Radiology Experimental, 2021, 5, 38.	1.7	20
53	Advanced Modeled Iterative Reconstruction in Low-Tube-Voltage Contrast-Enhanced Neck CT: Evaluation of Objective and Subjective Image Quality. American Journal of Neuroradiology, 2016, 37, 143-150.	1.2	19
54	ECG-gated Versus Non-ECG-gated High-pitch Dual-source CT for Whole Body CT Angiography (CTA). Academic Radiology, 2016, 23, 163-167.	1.3	19

#	Article	IF	CITATIONS
55	Gender differences in the diagnostic performance of machine learning coronary CT angiography-derived fractional flow reserve -results from the MACHINE registry. European Journal of Radiology, 2019, 119, 108657.	1.2	19
56	Systematic Comparison of Reduced Tube Current Protocols for High-pitch and Standard-pitch Pulmonary CT Angiography in a Large Single-center Population. Academic Radiology, 2016, 23, 619-627.	1.3	18
57	CT coronary calcium scoring with tin filtration using iterative beam-hardening calcium correction reconstruction. European Journal of Radiology, 2017, 91, 29-34.	1.2	18
58	Coronary Computed Tomography Angiography–Derived Plaque Quantification in Patients With Acute CoronaryÂSyndrome. American Journal of Cardiology, 2017, 119, 712-718.	0.7	18
59	Comparison of Radiation Dose and Image Quality of Contrast-Enhanced Dual-Source CT of the Chest: Single-Versus Dual-Energy and Second-Versus Third-Generation Technology. American Journal of Roentgenology, 2019, 212, 741-747.	1.0	18
60	Diagnostic accuracy of color-coded virtual noncalcium dual-energy CT for the assessment of bone marrow edema in sacral insufficiency fracture in comparison to MRI. European Journal of Radiology, 2020, 129, 109046.	1.2	17
61	Iterative beam-hardening correction with advanced modeled iterative reconstruction in low voltage CT coronary calcium scoring with tin filtration: Impact on coronary artery calcium quantification and image quality. Journal of Cardiovascular Computed Tomography, 2017, 11, 354-359.	0.7	16
62	Incremental diagnostic value of color-coded virtual non-calcium dual-energy CT for the assessment of traumatic bone marrow edema of the scaphoid. European Radiology, 2021, 31, 4428-4437.	2.3	16
63	Coronary artery assessment using self-navigated free-breathing radial whole-heart magnetic resonance angiography in patients with congenital heart disease. European Radiology, 2018, 28, 1267-1275.	2.3	15
64	Measurement Reliability and Diagnostic Accuracy of Virtual Monoenergetic Dual-Energy CT in Patients with Colorectal Liver Metastases. Academic Radiology, 2020, 27, e168-e175.	1.3	15
65	Accuracy and precision of volumetric bone mineral density assessment using dual-source dual-energy versus quantitative CT: a phantom study. European Radiology Experimental, 2021, 5, 43.	1.7	15
66	Dual-energy computed tomography in patients with cutaneous malignant melanoma: Comparison of noise-optimized and traditional virtual monoenergetic imaging. European Journal of Radiology, 2017, 95, 1-8.	1.2	14
67	Contrast media injection protocol optimization for dual-energy coronary CT angiography: results from a circulation phantom. European Radiology, 2018, 28, 3473-3481.	2.3	11
68	Current and future applications of CT coronary calcium assessment. Expert Review of Cardiovascular Therapy, 2018, 16, 441-453.	0.6	11
69	Value of minimum intensity projections for chest CT in COVID-19 patients. European Journal of Radiology, 2021, 135, 109478.	1.2	11
70	Quiet MR sequences in clinical routine: initial experience in abdominal imaging. Radiologia Medica, 2017, 122, 194-203.	4.7	10
71	Carotid and cerebrovascular dual-energy computed tomography angiography: Optimization of window settings for virtual monoenergetic imaging reconstruction. European Journal of Radiology, 2020, 130, 109166.	1.2	9
72	Impact of Intravenously Injected Contrast Agent on Bone Mineral Density Measurement in Dual-Source Dual-Energy CT. Academic Radiology, 2022, 29, 880-887.	1.3	9

MORITZ H ALBRECHT

#	Article	IF	CITATIONS
73	Evaluation of a Computer-Aided Diagnosis System for Automated Bone Age Assessment in Comparison to the Greulich-Pyle Atlas Method. Journal of Computer Assisted Tomography, 2019, 43, 39-45.	0.5	7
74	Radiation Optimized Dual-source Dual-energy Computed Tomography Pulmonary Angiography. Academic Radiology, 2017, 24, 13-21.	1.3	6
75	Cardiac Dual-Energy CT Applications and Clinical Impact. Current Radiology Reports, 2017, 5, 1.	0.4	5
76	Beam-hardening in 70-kV Coronary CT angiography: Artifact reduction using an advanced post-processing algorithm. European Journal of Radiology, 2018, 101, 111-117.	1.2	5
77	Quantitative inversion time prescription for myocardial late gadolinium enhancement using T1-mapping-based synthetic inversion recovery imaging: reducing subjectivity in the estimation of inversion time. International Journal of Cardiovascular Imaging, 2018, 34, 921-929.	0.7	4
78	Long-term outcomes following percutaneous microwave ablation for colorectal cancer liver metastases. International Journal of Hyperthermia, 2022, 39, 788-795.	1.1	4
79	Nonbinary quantification technique accounting for myocardial infarct heterogeneity: Feasibility of applying percent infarct mapping in patients. Journal of Magnetic Resonance Imaging, 2018, 48, 788-798.	1.9	3
80	New Imaging Techniques for Atherosclerotic Plaque Characterization. Current Radiology Reports, 2017, 5, 1.	0.4	2
81	Dual-Energy CT for analyzing extracellular volume fraction: A promising novel technique in myocardial fibrosis diagnostics?. Journal of Cardiovascular Computed Tomography, 2020, 14, 377-378.	0.7	2
82	Low-dose CT pulmonary angiography on a 15-year-old CT scanner: a feasibility study. Acta Radiologica Open, 2016, 5, 205846011668437.	0.3	1
83	Coronary CT-Derived Fractional Flow Reserve. Current Radiology Reports, 2017, 5, 1.	0.4	0
84	Value of Latest-generation Cone-beam Computed Tomography for Post Lipiodol-embolization Imaging in Hepatic Transarterial Chemoembolization in Comparison with Multi-detector Computed Tomography. Academic Radiology, 2021, , .	1.3	0